POWERTRAIN SIZING FOR AN OFF-ROAD VEHICLE

Bianca Chaves Esteves, bianca.est2@hotmail.com [1]
Luís Vitor Martins Peres, lvitormps@gmail.com [1]
Lucas Marins Assunção, lucas.marins1994@gmail.com [1]
Lucas de Oliveira Lima, lucasoliveiralima98@gmail.com [1]
Jorge Franklin Mansur Rodrigues Filho, jorge.franklin.m@hotmail.com [1]
Alberto Paiva, albertopaiva@id.uff.br [1]

[1] Universidade Federal Fluminense – Volta Redonda School of Engineering – Department of Mechanical Engineering
420 Trabalhadores Av. – Volta Redonda − RJ – Brazil – 27.255-125

Abstract:. *Powertrain design is a well-established subject in the literature; nevertheless, its application should be sized according to the vehicle requirement. Depending on that, usual standard directions and bibliographic designing recommendations may not apply to multipurpose extreme demands, such as in off-road vehicles. Within this context, this paper focuses on the design methodology and numerical simulation of a powertrain system for an off-road BAJA type vehicle, taking into account the track tests requirements specified for BAJA SAE Brasil competition. The selected driveline involves a commercial Continuously Variable Transmission (**CVT**), followed by a fixed-reduction gearbox, handmade designed for this specific application. The proposed archetype should combine high torque to overcome severe obstacles with strong acceleration and final speed during the endurance test. Initially, a longitudinal dynamics analysis is conducted, taking into account the technical information of both engine and **CVT**, together with the vehicle performance requirements, in order to determine the optimal reduction ratio of the gearbox to explore the desired engine power range. The next step concerns the gearbox design, which comprises two tasks: design setup with the respective analytical calculations involving fatigue analysis of shafts and gears to obtain the desired reduction ratio and numerical simulation of these machine components, using computer-aided designing tools. The simulations consider static finite element stress analysis for them, based on the previous analytical design calculations, performed in ANSYS®. Performance results attest a balanced power transmission, in view of the above-cited contrasting demands.*

Keywords: *Powertrain; off-road vehicle; design methodology.*

1. INTRODUCTION

Automobile powertrain (also called driveline or drivetrain) comprises all components responsible for transmitting the power generated by the engine to the driving wheels – namely: gearbox, differential, transmission shafts, among other small parts (Jasuja et al. 1984).

There are different possible layouts for powertrain design, besides different transmission types. Several authors discuss these possibilities, such as: Dopson et al. (1995); Bombarda et al. (2000) and Georgiou & Haritos (2012). A typical classification is adopted in the literature (Naunheimer et al. 2011), for instance: manual gearbox transmission, automatic gearbox transmission and continuously variable transmissions (**CVT**). Following, each of them is briefly discussed.

A manual gearbox transmission, in its simpler concept, consists of an input shaft connected to the engine crankshaft, which is coupled (through a pair of gears) to a layshaft containing gears of different number of teeth. The number of gears in this layshaft defines the n-speed of the manual transmission. Under the command of a gear selector – generally, a hand lever – the user decides manually which gear of the layshaft should be engaged with the driven gear of the output shaft going forward to the driving wheels. There is a releasing system that enables gears interchange – the clutch – that should be actuated by the user as well. This system is considered robust (withstands high torque loads), with easy maintenance and enables engine break. On the other hand, it is little comfortable for users.

The automatic gearbox transmission emerged from the desire of gear shifting without the user interference. A main component should be added to the gearbox to enable this task – the torque converter – in substitution to the friction clutch. This device is composed by a turbine, a pump and an intermediate stator, with a fluid (the own transmission oil) flow inside that impels the turbine, whose shaft is connected to the gearbox input shaft, in order to amplify the engine torque transfer. The gearbox itself uses a system of planetary gears to select the appropriate gearing. In the very beginning, the torque converter was exclusively driven by both the engine rotation and the hydraulic fluid flow. This system presents two main drawbacks: it is expensive and introduces a transmission lag. As time passed by, electronic control was incorporated to the system (Kuroyanagi & Hattori 1984; Hrovat & Powers 1990), monitoring the pertinent parameters and, thus, reducing this transmission lag. Electronic control is used to optimize engine torque as well; for instance, Haider & Griffin (1987) propose a torque management control scheme to adapt high performance engines to commercial vehicles using automatic transmission.

Sometime later, after electronic control popularization (Narumi et al. 1990; Dorey et al. 1995; Bai et al. 2010), the automakers started to use this embedded electronic to command regular gearboxes – with clutches instead of the torque converter – aiming to save costs. This system became known as semi-automatic transmission, in which the user should

handle a gear selector, without commanding the clutch. Although this system seems to be effective (once everything is electronically controlled), the monitored parameters still depend on the user's way of driving. To avoid jerky gearshifts and even gearbox breakdown, the system operates slowly; therefore, the transmission lag arose again. In the recent years, a new technology was proposed to overcome this inconvenient. A dual-clutch system was incorporated to the gearbox (Walker et al. 2011). One clutch controls the odd-numbered gears, while the other controls the even-numbered gears. While varying the engine rotation, the gearbox lines up the next and the previous gears with the available clutch. According to the engine demand – whether the user wants to slow down or accelerate – the system simply switches from one clutch to the other. All this process is electronically controlled. This technology is being gradually implemented in commercial vehicles; therefore, its reliability is still unknown.

Another type of fully automatic transmission is the continuously variable transmission (**CVT**), which has been motivating research interest (Kluger & Fussner 1997; Patel et al. 2005). This system mainly consists of two bipartite conical sheaves, each of them with a sliding halve – that enable their diameter tunable – and a push-belt connecting them. The adjustable diameter of both sheaves propitiates a continuous variation of the transmission ratio (input from engine/output forward to the driving wheels). The transmission ratio range may be defined in order to explore the desired band of the engine rotation speed in the torque-power curve of the engine (performance *versus* economy), which allows a nearly constant rotation speed in the **CVT** input shaft, within the selected band. The actuation system to shift the moveable tier of each sheave may be activated either by centrifugal (roller) weights, whose movement is due to sheaves' rotation speed (for light vehicles with low torque transmission, such as scooters) or by oil pressure provided by a hydraulic line equipped with an oil pump (for vehicles requiring reliability due to high torque transmission such as commercial automobiles). The main drawback of this system relies on belt wear. Again, a distinction is made between the two applications – in general, rubber belts are adopted for low torque applications, while steel belts are adopted for high torque applications.

Nowadays, the hybrid and the fully electric vehicles are becoming popular. The electrical power supply (in thesis) does not demand a powertrain reduction system, since there is no problem with the generated rotation speed. However, some modern studies (Bayindir et al. 2011; Karimi et al. 2016) attest that the electric vehicle performance may be optimized with the inclusion of a variable ratio transmission.

The possibilities for the gearbox set have been addressed in the previous paragraphs; nevertheless, as pointed out earlier, there are some other components in the driveline to complete the assemblage such as: differential, constant-velocity (homokinetic) joints and transmission shafts. These components may be combined appropriately to provide the powertrain design layout. For each application, there is a vast range of possible combinations for the reduction (or even magnification, depending on purpose) of the rotation speed ratio input/output, in order to fulfill the vehicle requirements. Some authors dedicate attention to powertrain modeling and simulation, for example: Hrovat & Tobler (1991); Lomonaco et al. (2007) and Barak et al. (2011), while others are focused on comfort patterns, such as noise and vibration control (Shangguan et al. 2016).

Since powertrain started to be applied to vehicles in the beginning of the 20th century, this technology has evolved a lot and standard directions have been created (for instance: ISO, AGMA, among others) to rule powertrain design. However, these standard directions may not be exactly suitable for multipurpose extreme demands, such as in off-road vehicles, where the proposed archetype should combine high torque with strong acceleration, besides robustness to provide reliability.

Within this context, this article presents the powertrain sizing for an off-road BAJA type vehicle, which combines a commercial **CVT** transmission with a proposed fixed-reduction gearbox. Initially, the longitudinal dynamics analysis helps finding an optimal reduction ratio for the gearbox. After that, the gearbox constructive design is conceived and calculated to produce this desired reduction ratio, together with a fatigue analysis of shafts and gears to estimate their lifetime and; at last, numerical simulations for stress analysis through finite element method are performed for these components.

2. LONGITUDINAL DYNAMICS

This section focuses on longitudinal dynamics analysis, aiming to tune up the reduction ratio of the gearbox, towards engine power optimization. Based on technical information of both engine and **CVT** (which helps setting the input parameters of the gearbox), together with some vehicle performance requirements (parameters expected to be obtained from the output of the gearbox, taking into account the sources of energy loss), an iterative calculation process is conducted to find an optimal reduction ratio for the gearbox.

As stated before, the vehicle transmission combines a commercial **CVT** transmission with a fixed-reduction gearbox. The **CVT** model used is the "Gaged GX9", with a ratio reduction (input/output) ranging from $0.9:1$ up to $3.9:1$, with a rubber belt, usually applied in snow sleds, scooters/small motorcycles and some kinds of all terrain vehicles (**ATV**). The vehicle is powered by a Briggs & Stratton 10HP engine (Model: 20S232; Type: 0036-F1), which is typically applied in lawn mower and pressure washers.

According to the vehicle application, its performance has to consider a balance between torque and power; thus, from empirical results obtained through experimental tests of other similar prototypes, the following requirements should be fulfilled:

- Provide a minimum tractive force on driving wheels of 1680 N;
- Reach a minimum acceleration of 3.25 m/s^2 in 30 m;
- Reach a minimum speed of 44 km/h in 100 m.

The tractive force TF on driving wheels, for a rest condition, may be obtained, as follows (Gillespie, 1992; Heisler, 2002):

$$TF = EF - IRF \tag{1}$$

where EF is the force provided by the engine torque, while IRF encompasses all inertial resistance of rotating components of the drivetrain, given by:

$$EF = \frac{T_e\, N}{r}\,\eta\,; \qquad IRF = \frac{I^*\, N^2}{r^2}\,a_x \qquad \Rightarrow \qquad TF = EF - IRF = \frac{T\, N}{r}\,\eta - \frac{I^*\, N^2}{r^2}\,a_x \tag{2}$$

where: T_e is the output engine torque on its crankshaft; N is the overall reduction ratio (considering the superposition of both the **CVT** and the gearbox); r is the radius of the wheel set (including the tire); η is the overall transmission efficiency (considering all components involved); I^* is the overall mass moment of inertia of all rotating components of the drivetrain;

Then, the equation of motion describing the vehicle longitudinal dynamics can be evaluated using *Newton*'s *Second Law* in its scalar form for "x" direction, such that:

$$\sum F_x = m\,a_x \qquad \Rightarrow \qquad TF - ADF - RRF = m\,a_x \tag{3}$$

where: F_x corresponds to the overall forces acting upon the vehicle in the longitudinal "x" direction; m is the vehicle mass; a_x is the vehicle longitudinal acceleration; TF is the net tractive force on driving wheels; ADF is the aerodynamic drag force, while RRF represents the rolling resistance forces, without considering tire slipping.

The dissipation forces provided by ADF and RRF may be evaluated as follows (Naunheimer et al. 2011):

$$ADF = \frac{\rho_A\, c_x\, A\, v^2}{2}; \qquad RRF = m\,g\,\mu \tag{4}$$

where: ρ_A is the air mass density; c_x is the aerodynamic drag coefficient; A is the total frontal area of the vehicle; v is the vehicle longitudinal speed; g is the acceleration due to gravity and μ is the static friction coefficient.

Finally, substituting the expressions given by Eqs. (2) and (4) in the equation of motion (Eq. 3), leads to:

$$EF - IRF - ADF - RRF = m\,a_x \qquad \Rightarrow \qquad \frac{T_e\, N}{r}\,\eta - \frac{I^*\, N^2}{r^2}\,a_x - \frac{\rho_A\, c_x\, A\, v^2}{2} - m\,g\,\mu = m\,a_x \tag{5}$$

With Eq. (5) in hand, the next step is to find the optimal reduction ratio for the gearbox, recalling that the reduction ratio N considered in this expression takes into account the cumulative reduction provided by both the **CVT** and the gearbox. Nevertheless, the intricate point to achieve this goal is that the **CVT** reduction ratio depends on the output rotation speed of the engine crankshaft (which, in turn, has to do with the longitudinal speed v, since the gearbox reduction ratio is fixed). Besides that, it is necessary to fulfill the vehicle performance requirements that are set above, involving tractive force, speed and acceleration. As a conclusion, this calculation demands an iterative procedure.

Concerning the necessary parameters to be identified, some of them are known from the literature, such as: ρ_A and g. Others can be directly measured in the vehicle, such as: r, I^*, A and m, while the remaining parameters – namely: T_e, η, c_x and μ should be evaluated more carefully as follows.

From the manufacturer torque curve present in Fig. 1, the maximum output engine torque T on its crankshaft is estimated. Concerning the transmission efficiency, the parameter η is reported in the literature between 0.8 and 0.9; therefore, for this work, some efficiency loss is adopted in the rubber push-belt of the **CVT**. The aerodynamic drag coefficient c_x is estimated through a computational fluid dynamics (**CFD**) analysis in ANSYS®, considering a constant vehicle longitudinal speed of 50 km/h (including the driver's mass), against a wind flow of 22 km/h. Tires' manufacturer catalogs provide an average static friction coefficient μ for **ATV**s.

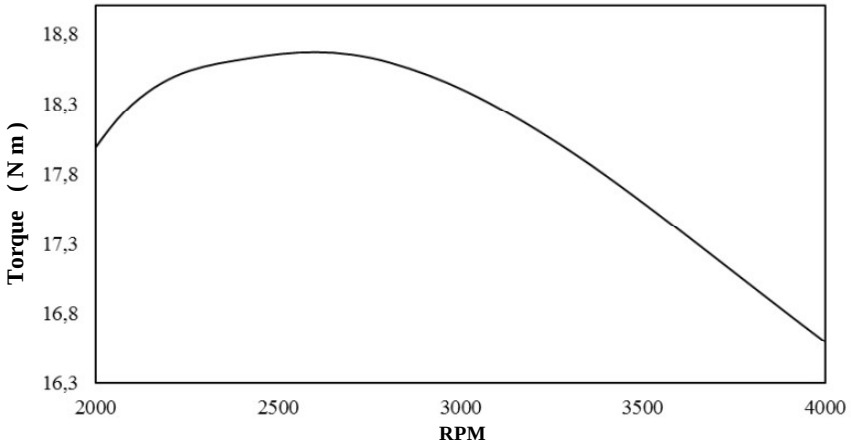

Figure 1. Torque curve for Briggs & Stratton 10HP engine.

All necessary parameters to evaluate the reduction ratio for the gearbox (Eq. 5) are displayed in Tab. 1.

Table 1. Parameters for longitudinal dynamics analysis.

T_e (Nm)	r (m)	η	I^* (kg m^2)	ρ_A (kg m^{-3})
18	0.53	0.89	3.79	1.2
c_x	A (m^2)	m (kg)	g (m s^{-2})	μ
1.32	1.77	230	9.81	0.015

During the iterative procedure, simultaneous speed and acceleration curves are investigated as a function of time for different gearbox reduction ratios. After adapting the available parameters to fulfill the desired vehicle performance requirements, an optimized reduction ratio of 7.18:1 is adopted for the gearbox.

Figure 2 shows the tractive force response for different regimes (low gear and fast gear) together with the **CVT** performance curve and the available engine power as a function of longitudinal speed of the vehicle. The analysis attests that, for low speed levels (< 10 km/h) where the traction force is strongly demanded, the original requirement of $TF \geq 1680$ N is fulfilled.

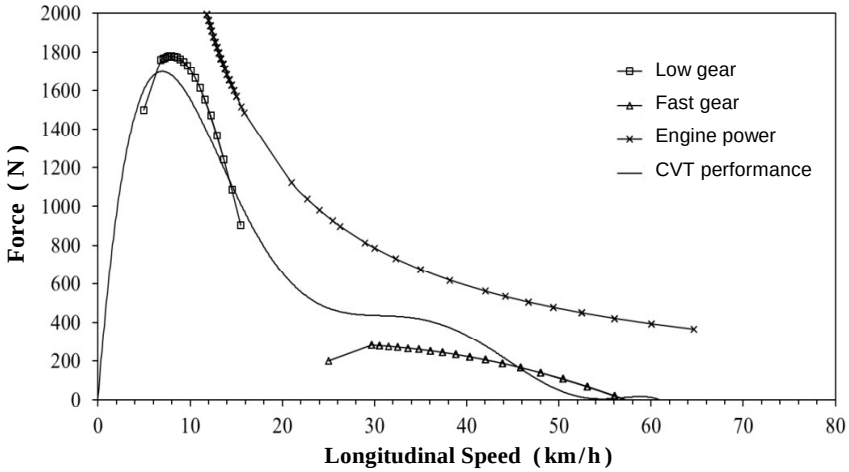

Figure 2. Tractive force and CVT performance.

3. GEARBOX DESIGN

This section involves two subsections, as follows. The first one considers the analytical design calculations to obey the desired reduction ratio, together with the fatigue analysis of shafts and gears to estimate their lifetime. The second one presents static finite element stress analysis for these components, using ANSYS®.

3.1. Analytical Calculations and Fatigue Analysis

This subsection is mainly dedicated to the design of the machine components responsible for the gearbox transmission, regarding their fatigue analysis. Moreover, some other complementary features are addressed, such as: material selection, bearings and seals specification and lubricating system description. A two-stage reduction is adopted, involving three shafts and two pairs of spur gears, chosen for both their simplicity and their cost benefit. They are sized according to ANSI/AGMA standard, undergoing von Mises failure criterion, while the shafts are sized according to ANSI/ASME standard together with Soderberg fatigue criterion.

At first, a geometric layout is proposed based upon the available space to settle the gearbox in the vehicle (for more details about the constructive characteristic of the complete gearbox, please refer to Chaves & Paiva (2017). This architecture is the starting point to define the main parameters of machine components. For instance, the diameters of the three shafts are evaluated through Eq. (6), as follows (Budynas & Nisbett 2014):

$$d \geq \sqrt[3]{\frac{32\sqrt{M^2 + 0.75T^2}}{\pi \sigma_y}} \tag{6}$$

where: d is the shaft diameter; M is the maximum bending moment to which the shaft is submitted, T is the input torque at each shaft and σ_y is the yielding stress.

The endurance stress limit at the critical location of a machine part in the geometry and condition of use S_e' should be adjusted by some geometric and environmental factors, in order to provide a more realistic endurance stress limit forecast. Equation (7) shows the common factors used in this kind of analysis (Ugural, 2003,2015; Juvinall & Marsheck, 2011; Norton 2011, 2013; Budynas & Nisbett, 2014).

$$S_e = K_a K_b K_c K_d K_e S_e^{'} \tag{7}$$

where: S_e is the adjusted endurance limit, while K_a, K_b, K_c, K_d and K_e are the *Marin* factors applied to the endurance limit that will be later explained.

Rotating equipment may be submitted to time-varying loads (that cause time-varying stress states); thus, an alternate stress history (here denoted by σ_a) may be superimposed to a constant mean stress σ_m. Equation (7) sets a safety factor regarding these cumulative different sources of stress.

$$S_f = \left(\frac{\sigma_a}{S_e} + \frac{\sigma_m}{\sigma_y} \right)^{-1} \tag{8}$$

Table 2 summarizes the main parameters and results used in the shafts' design, recalling that they are machined from a SAE 4340 Steel stem. Considering these parameters, the reduction ratio for the first pair of gears results in 1.76:1; while, for the second, the ratio provides 1.6:1.

The spur gears are designed, according to AGMA standards, for finite fatigue life of 10^5 cycles. Thus, the bending stress on the gear tooth denoted by s and the contact stress due to pitting denoted by s_c are given as follows, by Eq. (9), while the safety factors, being one against bending fatigue failure and the other against pitting wear failure – S_F and S_H respectively, are given by Eq. (10).

$$s = W^t K_o K_v K_s \frac{P_d}{F} \frac{K_m K_B}{J}; \qquad s_c = C_p \left(W^t K_o K_v K_s \frac{K_m}{d_P F} \frac{C_f}{I} \right)^{0.5} \tag{9}$$

$$S_F = \frac{S_t Y_N}{s K_T K_R}; \qquad S_H = \frac{S_c Z_N C_H}{s_c K_T K_R} \tag{10}$$

After an iterative process involving Eqs. (9) and (10), aiming to save weight, the final results obtained are listed in Tab. 3, together wit the necessary parameters.

Table 2. Parameters for fatigue analysis of gearbox shafts.

	Input shaft	Layshaft	Output shaft
Maximum bending moment – M (N m)	152.6	163.0	354.0
Shaft diameter (mm)	20	25	30
Input torque – T (N m)	70.20	210.60	547.56
Alternate stress – σ_a (Mpa)	66.29	35.96	45.63
Equivalent mean stress – σ_m (MPa)	149.61	138.12	199.33
Safety Factor – S_f	1.62	2.24	1.63
Yielding limit – σ_y (MPa)	510		
Endurance limit – S_e' (MPa)	381.5		
Adjusted endurance limit – S_e (MPa)	204.9		
Surface condition modification factor – K_a	0.78		
Size modification factor – K_b	0.92		
Load modification factor – K_c	1		
Temperature modification factor – K_d	1		
Reliability factor – K_e	0.75		

Table 3. Parameters for sizing gearbox spur gears.

	1st Pair		2nd Pair	
Pitch diameter – d_P (mm)	50.0	138.0	60.0	156.0
Bending stress on the gear tooth – s (MPa)	337		412	
Contact stress due to pitting – s_c (MPa)	1401		1579	
Tangential transmitted load for maximum torque – W^t (N)	2808		7020	
Safety factor against bending fatigue failure – S_F	1.47		1.20	
Safety factor against pitting wear failure – S_H	1.69		1.50	
Transverse diameteral pitch – P_d	400		333	
Face width of the narrower member – F (mm)	15		25	
Surface-strength geometry factor – I	0.118		0.116	
Bending-strength geometry factor – J	0.342		0.35	
Surface condition factor – C_f	1.1			
Hardness-ratio factor – C_H	1			
Elastic coefficient – Cp ($MPa^{1/2}$)	191			
Overload factor – K_0	1			
Rim-Thickness Factor – K_B	1			
Load-distribution factor – K_m	1.1			
Reliability factor – K_R	0.9			
Size factor – K_s	1			
Temperature factor – K_T	1			
Dynamic factor – K_v	1.4			
Allowable bending stress number – S_t (MPa)	381.45			
Allowable contact stress number – S_c (MPa)	1643			
Stress Cycle Factor – Y_N	1.17			
Stress Cycle Factor – Z_N	1.30			

Table 4 shows complementary geometric features concerning the two gaging sets previously designed. Again, for more details about the complete gearbox, such as technical drawings, please refer to Chaves & Paiva (2017).

Table 4. Gear parameters.

Gear	Number of teeth	Contact Ratio	Module	Face width (mm)
Pinion 1	20	2.5	2.5	15
Bevel 1	55			
Pinion 2	20	3.8	3.0	25
Bevel 2	52			

Table 5 displays the flat keys dimensions (height, width and length). It is worthwhile to notice an increase in robustness from the input to the output shaft, with an increasing loading demand (see loads and stresses in Tab.2).

Table 5. Flat key dimensions.

Shaft	Height (mm)	Width (mm)	Length (mm)
Input shaft	6	6	10
Layshaft	8	7	10 (pinion) / 20 (bevel)
Output shaft	8	7	20

Figure 3(a) shows the exploded view of gearbox components designed in SolidWorks Co. All components are drawn in 3-D and the virtual assembling of the whole gearbox inhibits possible mismatches or interferences. Figure 3(b) shows a photograph of the manufactured gearbox prototype open, without one halve of the bipartite housing.

(a) **(b)**

Figure 3. Gearbox assembling.
(a) Exploded view of gearbox components designed in SolidWorks; (b) Photo of the gearbox prototype open.

Once the shafts' diameters are known (Tab. 2), it is possible to calculate/specify appropriate bearings and the seals. They are chosen from technical catalogs based on typical commercially found components that can be provided by different trademarks. Table 6 shows the selected bearings and seals for each shaft.

Table 6. Shaft diameters with respective bearings and seals.

Shaft	Diameters (mm)	Bearings	Seals
Input shaft	20	6004	00505BR
Layshaft	25	6205	–
Output shaft	30	6206	01535BR

Concerning lubrication, the gears remain partially immersed in oil, since the gearbox is placed almost in the vertical position and the oil level reaches the intermediate layshaft. Besides that, gears rotation speed ensures the oil flow inside the gearbox, sprinkling the superior shaft and gear. The adopted lubricating fluid is SAE 90 / GL-5, commonly applied in off-road transmissions.

At last, Tab. 7 presents the list of material selected for the gearbox components. All choices favor the cost benefit, without neglecting the mechanical design requirements, such as: yielding strength and hardness.

Table 7. Material specification for the gearbox components.

Component	Material	Heat Treating
Shafts	SAE 4340 Steel	Heating up to 1118 K; oil quenching; tempered at 503 K
Gears	SAE 8620 Steel	Oil quenching; tempered
Flat keys	SAE 4340 Steel	Heating up to 1218 K; oil quenching; tempered at 503 K
Housing	7075 Aluminun	T6

The 3-D geometry conceived in SolidWorks Co. is exported to ANSYS®, for a further stress analysis. Before that, in the pre-processing step, a static contact analysis is conducted, in order to verify the gears fitting. The static friction coefficient between two engaged teeth is 0.15. The viscous damping due to the oil underlying this pair of gears is neglected. Figure 4 illustrates the second pair of gears, where Fig. 4(a) shows the gears fitting analysis, while Fig. 4(b) presents the gear meshing in ANSYS®, using a 3-D structural solid "triangle 6-node 2" element type, with mesh refinement, due to both the flat keys regions and the gear teeth.

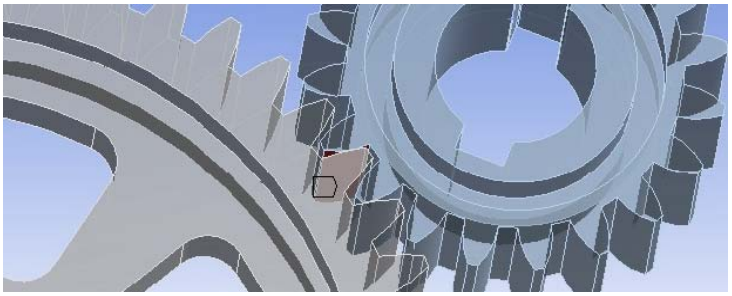

(a)

(b)

Figure 4. Gears fitting analysis and gear meshing for the second pair of gears in ANSYS®. (a) Gage/contact analysis; (b) Meshing.

3.2. Finite Element Stress Analysis

This subsection deals with the numerical simulations for stress analyses, involving shafts and gears, using ANSYS®. All gears and shafts are submitted to the stress analysis; nevertheless, this work presents only the critical situations, which take place in the output shaft as well as in the second pair of gears. The main target of these simulations is to identify critical regions of stress concentrations and the possibility of reducing mass in the gears.

All external loads (forces and torques) are prescribed for a critical situation, where the engine is accelerated passing through the engine rotation speed that supplies maximum torque for the input shaft (transmitted to the output shaft, according to the calculations developed in Section 3.1) and the breaks are activated blocking the wheels, completely restraining the brake disk support (circular disk of Fig. 6a) of the output shaft. Although this situation is improbable, it simulates the most critical loading condition acting on the assembling involving the second gear pair and the output shaft.

Figure 5 shows the finite element stress analysis in ANSYS® for the output shaft. Figure 5(a) shows the shaft meshing, using the same element type previously reported for the gears meshing. Figure 5(b) presents the stress response for the output shaft using the von Mises equivalent stress criterion. In general, the stress level results are below the expected calculated limit values of Section 3.1, except for the flat key region, where the second bevel is placed.

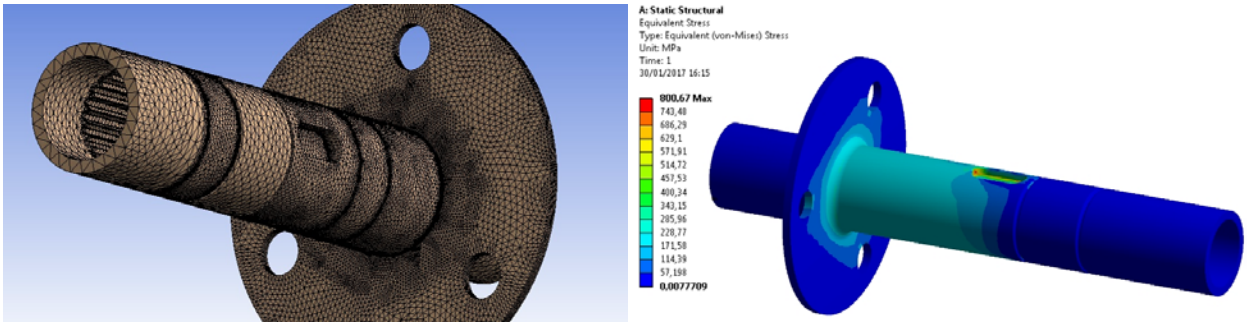

(a) **(b)**

Figure 5. Finite element analysis in ANSYS® for the gearbox output shaft.
(a) Meshing; (b) Stress analysis.

Figure 6 shows the finite element stress analysis in ANSYS® for the second pair of bevel-pinion set. Figure 6(a) presents the stress response for both gears using the von Mises equivalent stress criterion. Again, the stress level results are below the expected calculated limit values of Section 3.1, except for the flat key region in the pinion. Figure 6(b) shows a detail of the flat key slot of the pinion, where it is possible to identify very small regions with peak stresses. While manufacturing the prototype, a fillet radius is added in the internal part of the flat key slot to avoid this stress concentration.

(a)

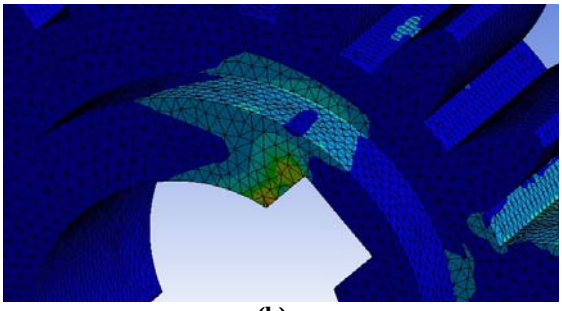

(b)

Figure 6. Finite element stress analysis in ANSYS® for the second pair of gears.
(a) Analysis of bevel-pinion set; (b) Detail of the flat key slot of the pinion.

4. CONCLUSIONS

This paper deals with the design methodology and numerical simulation of a powertrain system for an off-road vehicle. The proposed driveline combines a commercial **CVT** transmission with a proposed fixed-reduction gearbox. The longitudinal dynamics enables the identification of an optimal reduction ratio for the gearbox. The gearbox design provided the calculated estimations for the elements geometry and for load/stress limits that they can support, considering the appropriate fatigue factors. The numerical simulations for stress analyses, involving shafts and gears, attest the analytical calculations for the gearbox design, except for the flat key region, recalling that the simulations are performed for an almost unfeasible load condition and, besides that, there are still safety factors. Although it is beyond the scope of this work, a prototype of this gearbox has been manufactured and tested in an off-road vehicle with the aforementioned engine and **CVT** configurations, meeting both kinematical vehicle performance requirements set in the beginning of this work, with the following results: speed of 46.67 km/h in 100 m and acceleration of 3.215 m/s^2 in 30 m. From now on, the focus falls upon reliability.

5. REFERENCES

Bai, S., Brennan, D., Dusenberrry, D., Tao, X. & Zhang, Z.; 2010; "Integrated Powertrain Control"; SAE Technical Paper; Article N. 2010-01-0368; 7 pp.

Barak, A., Klir, V. & Cervenka, L.; 2011; "Powertrain Simulation Tool"; SAE Technical Paper; Article N. 2011-37-0027; 10 pp.

Bayindir, K., Gözüküçük, M. & Teke, A.; 2011; "A Comprehensive Overview of Hybrid Electric Vehicle: Powertrain Configurations, Powertrain Control Techniques and Electronic Control Units"; Energy Conversion and Management; Vol. 52; N. 2; pp. 1305–1313.

Bombarda, G., Gaviani, G. & Marceca, P.; 2000; "Powertrain System Design: Functional and Architectural Specifications"; SAE Technical Paper; Article N. 2000-01-C049; 13 pp.

Budynas, R.G. & Nisbett, J.K.; 2014; "Shigley's Mechanical Engineering Design"; Ed. McGraw Hill; 10th Ed.; 1104 pp.

Chaves, B.E. & Paiva, A.; 2017; "Technical Report for the 23rd Baja-SAE Brazil Competition"; Baja-SAE 2017 Proceedings; 17 pp.

Dopson, C., Taitt, D. & Sandford, M.H; 1995; "Powertrain Systems Definition Process"; SAE Technical Paper; Article N. 950811; 15 pp.

Dorey, R.E., Maclay, D., Shenton, A.T. & Shafiei, Z.; 1995; "Advanced Powertrain Control Strategies"; Advances in Automotive Control; pp. 151–156.

Georgiou, A. & Haritos, G.; 2012; "Advanced Phase Powertrain Design Attribute and Technology Value Mapping"; Sustainable Vehicle Technologies; pp. 47–57.

Gillespie, T.D.; 1992; "Fundamentals of Vehicle Dynamics"; Published by: Society of Automotive Engineers – SAE International; 470 pp.

Haider, S.A. & Griffin, J.A.; 1987; "Powertrain Torque Manager"; SAE Technical Paper; Article N. 870081; 8 pp.

Heisler, H.; 2002; "Advanced Vehicle Technology"; Ed. Butterworth-Heinemann; 2nd Ed.; 654 pp.

Hrovat, D. & Powers, W.F.; 1990; "Modeling and Control of Automotive Power Trains"; Control and Dynamic Systems; Vol. 37; pp. 33–64.

Hrovat, D. & Tobler, W.E.; 1991; "Bond Graph Modeling of Automotive Power Trains"; Journal of the Franklin Institute; Vol. 328; N. 5–6; pp. 623–662.

Igami, H., Thompson, M. & Osodo, K.; 2008; "Automative Powertrain Mounting System Design Optimization"; SAE Technical Paper; Article N. 2008-01-0879; 6 pp.

Jasuja, S.C., Perumalswami, P.R. & Borowski, V.J.; 1984; "Powertrain Structural Analysis"; SAE Technical Paper; Article N. 840742; 4 pp.

Juvinall, R.C. & Marsheck, K.M.; 2011; "Fundamentals of Machine Component Design"; Ed. John Wiley & Sons; 5th Ed.; 928 pp.

Karimi, H.R., Wang, R., Zhang, H. & Wang, J.; 2016; "Control and Estimation of Advanced Powertrains for Electrified Vehicles"; Mechatronics; Vol. 38; pp. 91–92.

Kluger, M. & Fussner, D.; 1997; "An Overview of Current CVT Mechanisms, Forces and Efficiencies"; SAE Technical Paper; Article N. 970688; 10 pp.

Kuroyanagi, J. & Hattori, T.; 1984; "Electronic Control of Automobile Powertrain"; SAE Technical Paper; Article N. 845094; 9 pp.

Lomonaco, J.P., DiValentin, E. & Back, M.; 2007; "Powertrain Modeling Advances"; SAE Technical Paper; Article N. 2007-01-1463; 12 pp.

Narumi, N., Suzuki, H. & Sakakiyama, R.; 1990; "Trends of Powertrain Control"; SAE Technical Paper; Article N. 901154; 11 pp.

Naunheimer, H., Bertsche, B., Ryborz, J. & Novak, W.; 2011; "Automotive Transmissions: Fundamentals, Selection, Design and Application"; Ed. Springer; 2nd Ed.; 717 pp.

Norton, R.L.; 2011; "Design of Machinery"; Ed. McGraw Hill; 5th Ed.; 857 pp.

Norton, R.L.; 2013; "Machine Design"; Ed. Pearson; 5th Ed.; 1104 pp.

Patel, D., Ely, J., & Overson, M.; 2005; "CVT Drive Research Study"; SAE Technical Paper; Article N. 2005-01-1459; 10 pp.

Shangguan, W., Liu, X., Lv, Z. & Rakheja, S.; 2016; "Design Method of Automotive Powertrain Mounting System based on Vibration and Noise Limitations of Vehicle Level"; Mechanical Systems and Signal Processing; Vol. 76–77; pp. 677–695.

Ugural, A.C.; 2003; "Mechanical Design – An Integrated Approach"; Ed. McGraw Hill; 832 pp.

Ugural, A.C.; 2015; "Mechanical Design of Machine Components"; Ed. CRC Press; 2nd Ed.; 1034 pp.

Walker, P.D., Zhang, N. & Tamba, R.; 2011; "Control of Gear Shifts in Dual Clutch Transmission Powertrains"; Mechanical Systems and Signal Processing; Vol. 25; N. 6; pp. 1923–1936.

6. RESPONSIBILITY NOTICE

The authors are the only responsible for the printed material included in this paper.